

Supporting Information

Morpholine modified Ru-based agents with multiple antibacterial mechanisms as metalloantibiotic candidates against *Staphylococcus aureus* infection

Shijie Lin^{a§}, Yun Song^{b§}, Yajuan Sun^{b§}, Wenjing Lin^b, Guangying Yu^b, Xiangwen Liao^b,

Qiang Yang^{c*}

[a] Department of Pharmacy, Hainan General Hospital (Hainan Affiliated Hospital of Hainan Medical University), Haikou, 570311, China

[b] Jiangxi Provincial Key Laboratory of Drug Design and Evaluation, School of Pharmacy, Jiangxi Science & Technology Normal University, Nanchang, 330013, China

[c] Department of Clinical Pharmacy, Hainan Cancer Hospital, Haikou, 570100, China

§ These authors contribute equally to this work

* Correspondence author:

Qiang Yang, E-mail: 18789551643@163.com

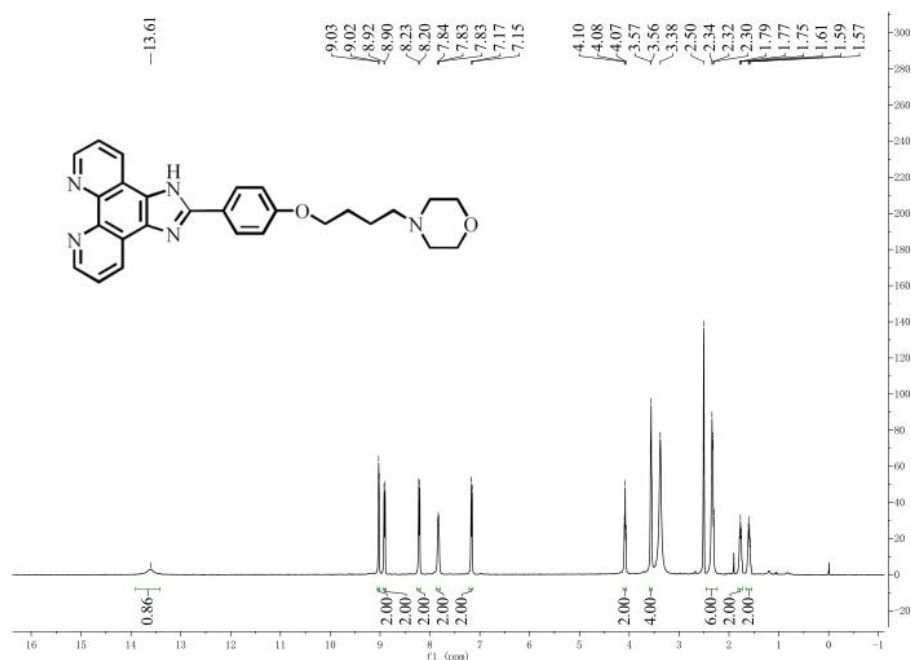


Figure S1. The ^1H NMR of MPLP ligand

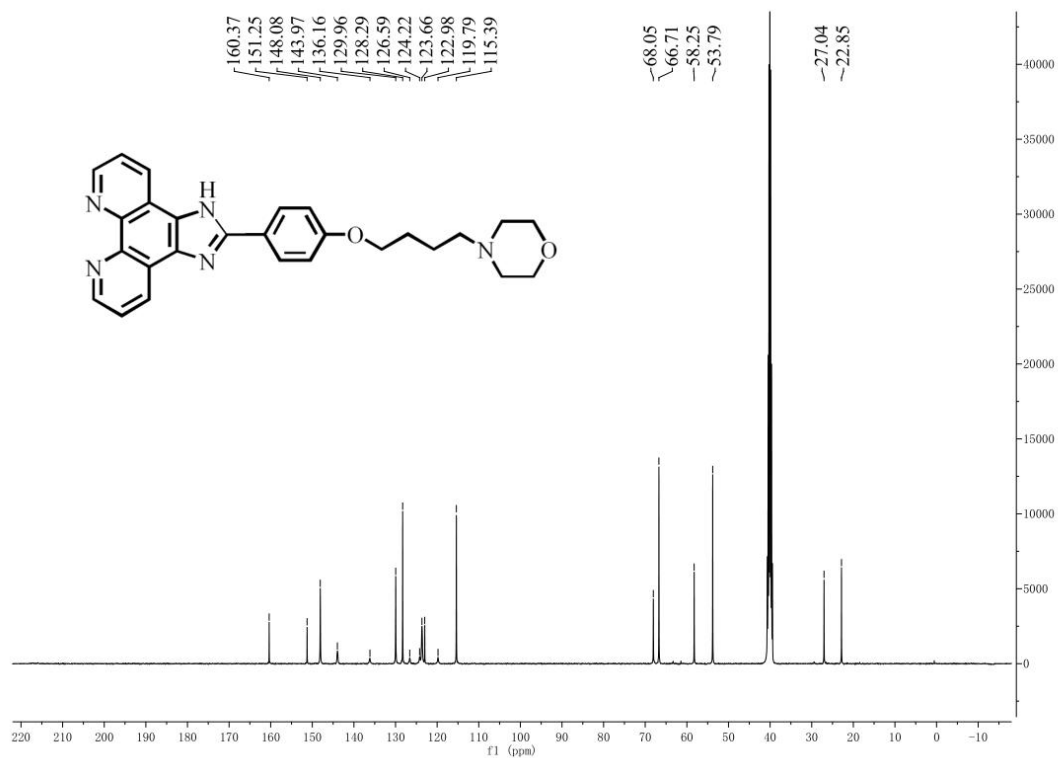


Figure S2. The ^{13}C NMR spectrum of the MPLP.

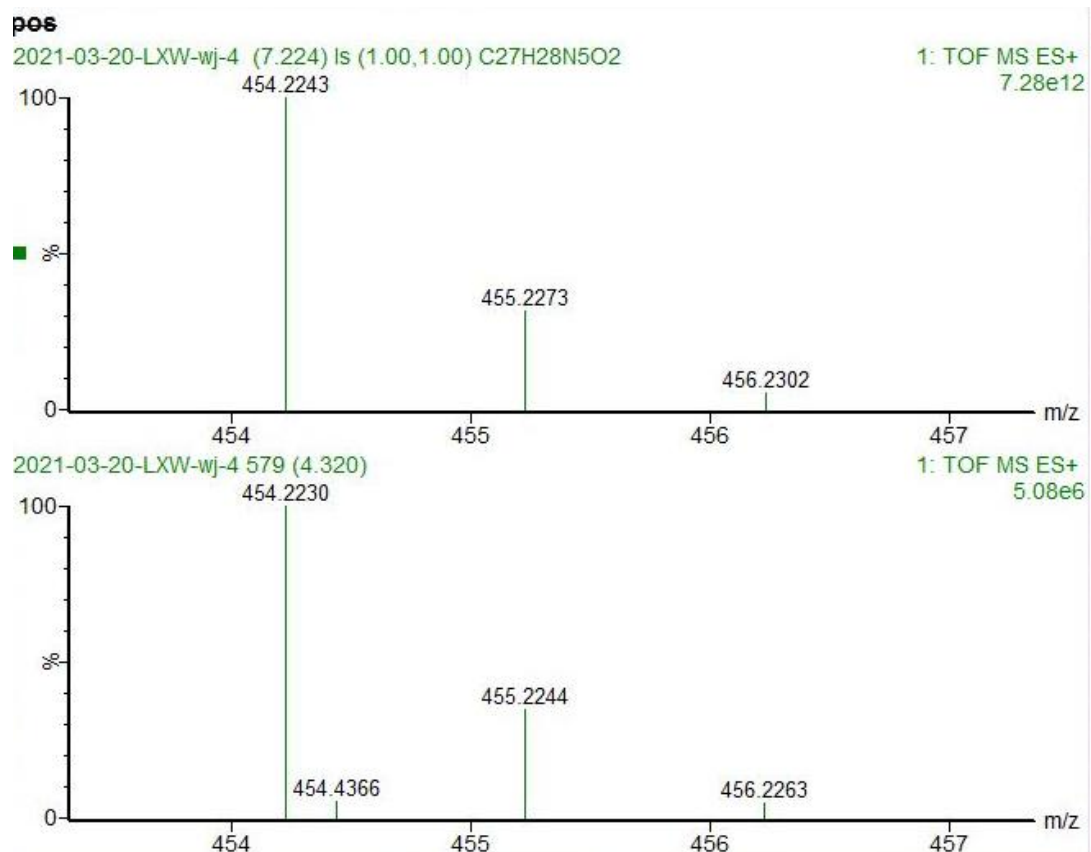


Figure S3. The HMRS of ligand MPLP.

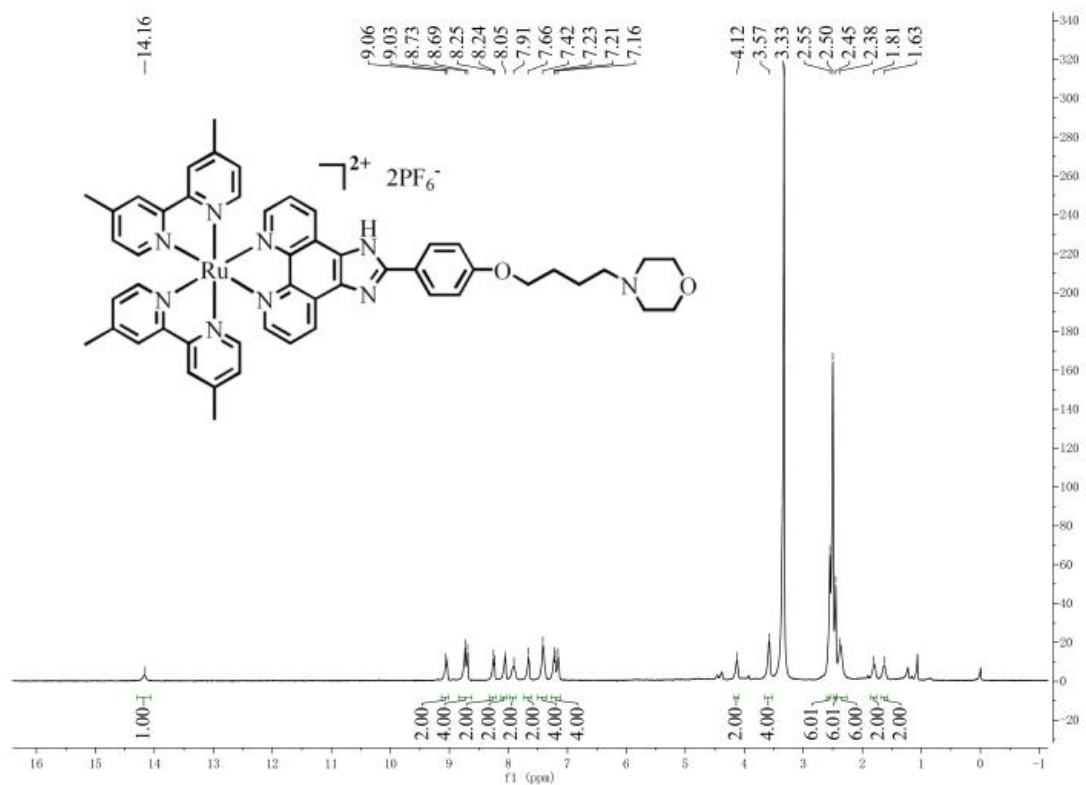


Figure S4. The ¹H NMR of Ru(II)-1.

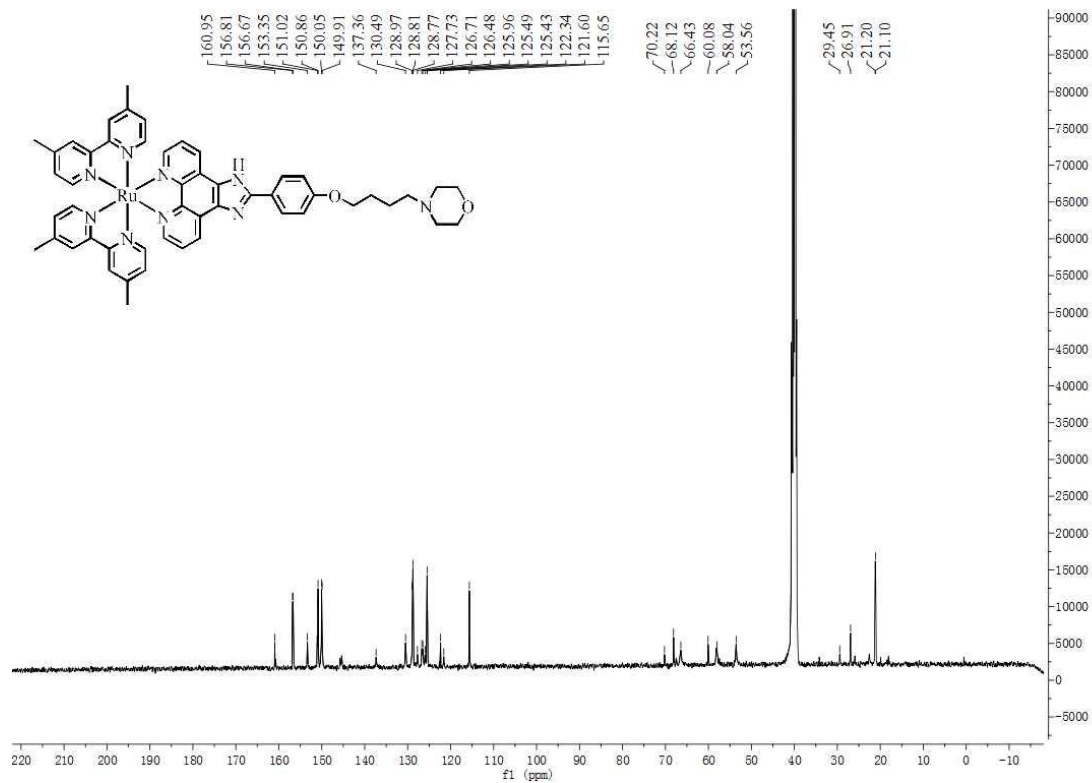


Figure S5. The ^{13}C NMR spectrum of the Ru(II)-1.

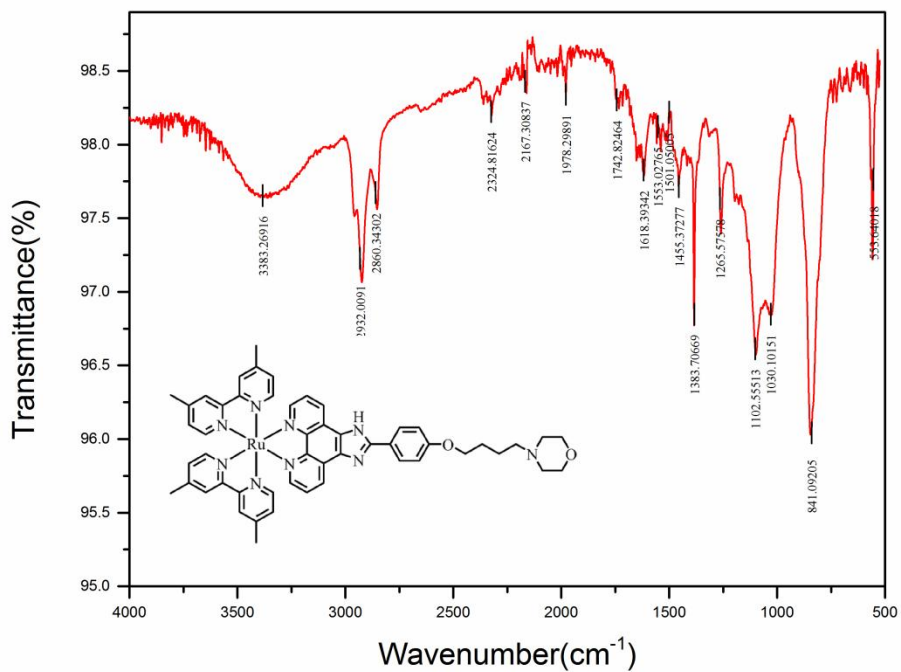


Figure S6. The IR spectrum of the Ru(II)-1.

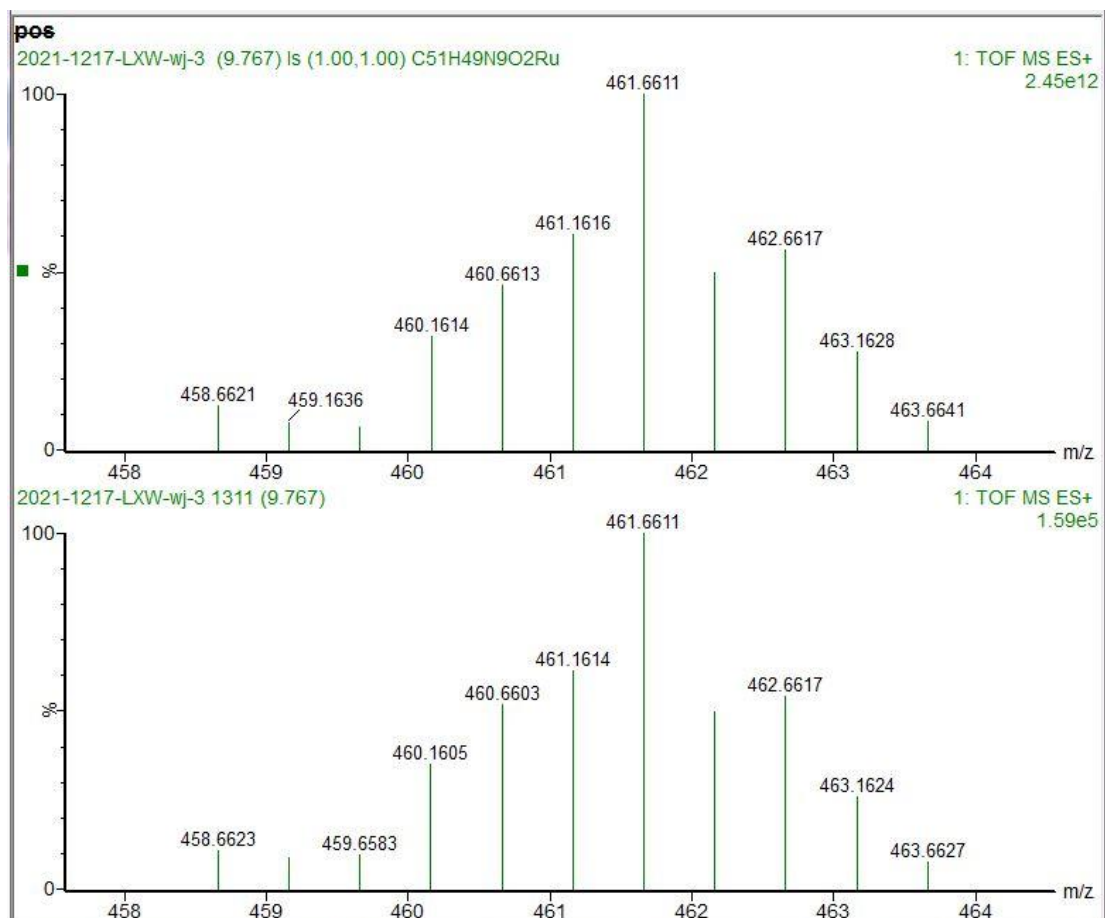


Figure S7. The HMRS of ligand **Ru(II)-1**.

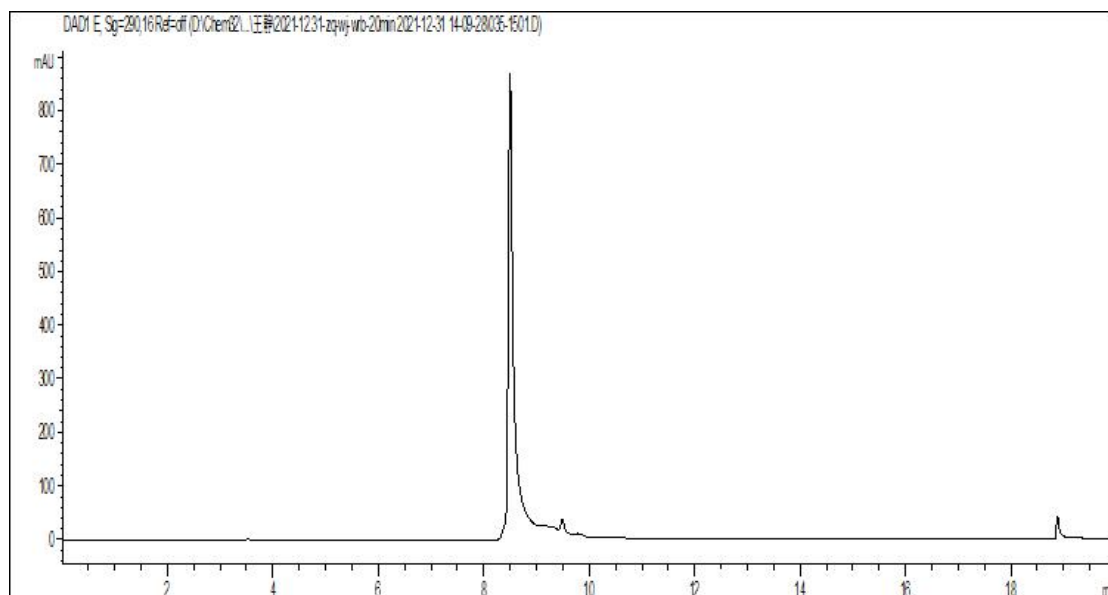


Figure S8. The HPLC of **Ru(II)-1**.

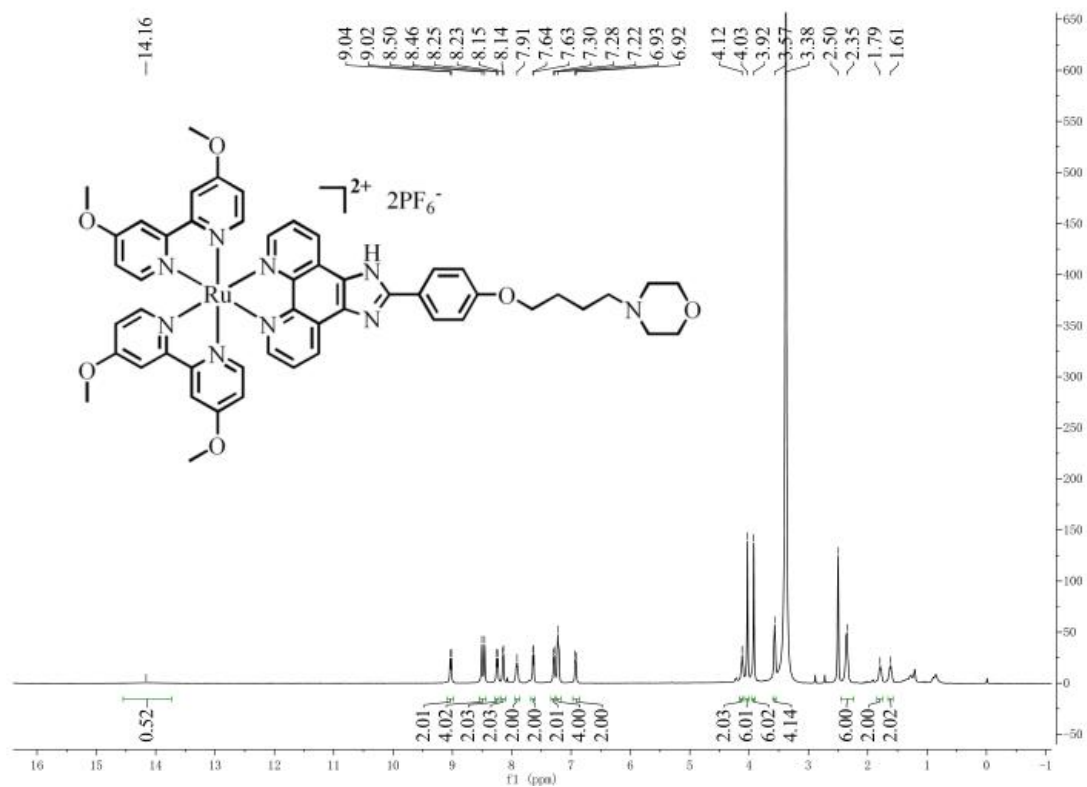


Figure S9. The ¹H NMR of Ru(II)-2.

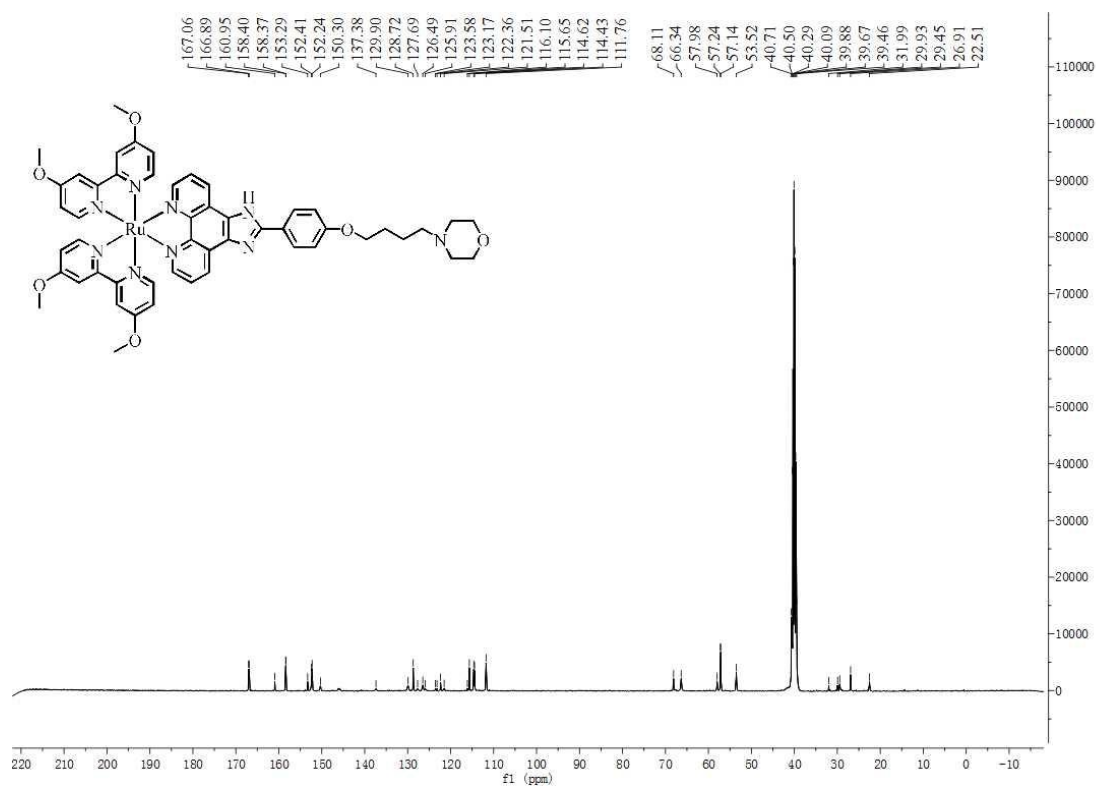


Figure S10. The ¹³C NMR spectrum of the Ru(II)-2.

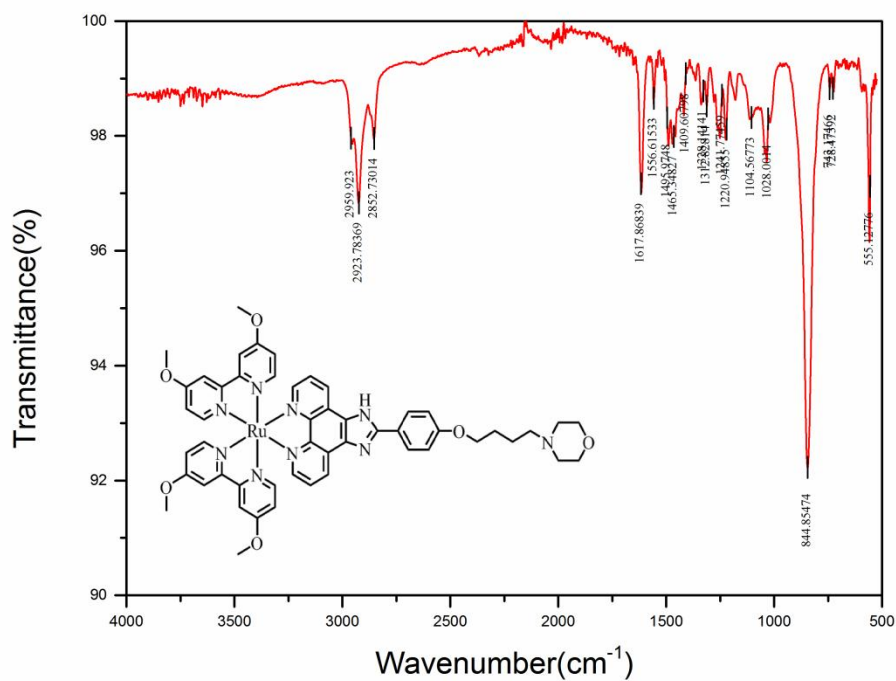


Figure S11. The IR spectrum of the Ru(II)-2.

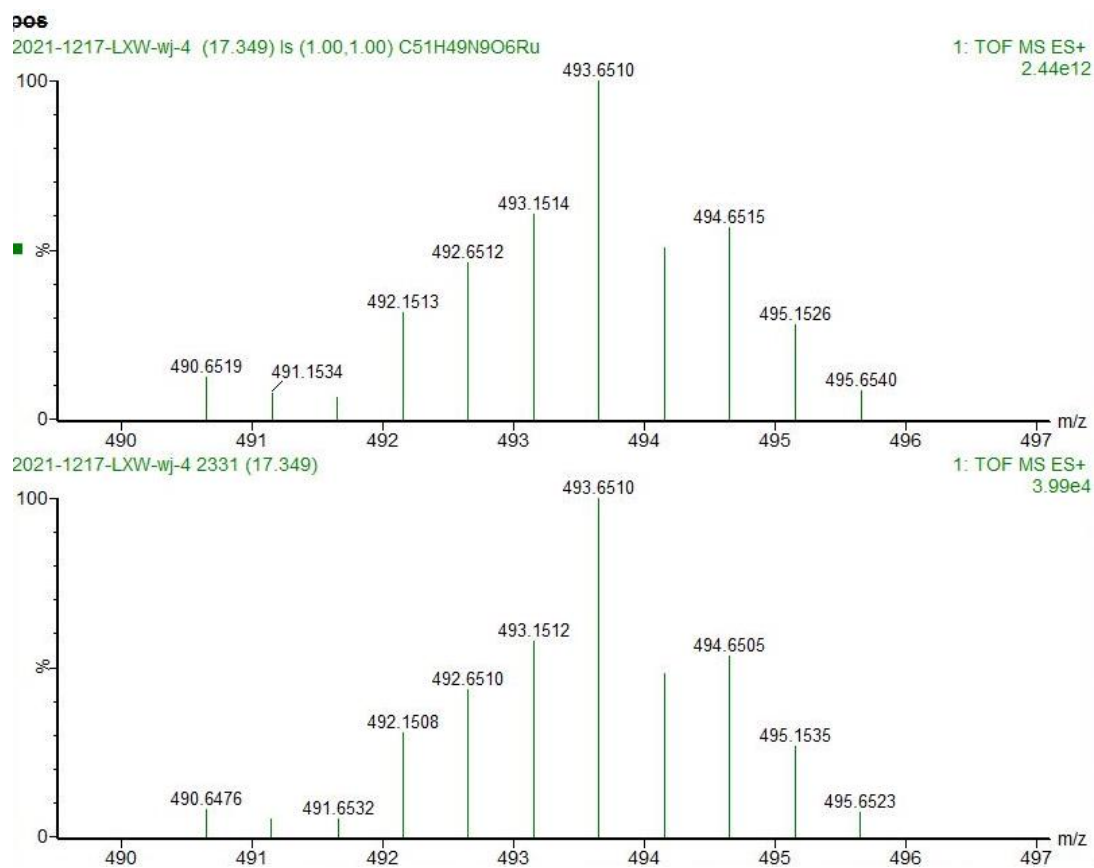


Figure S12. The HRMS of ligand Ru(II)-2.

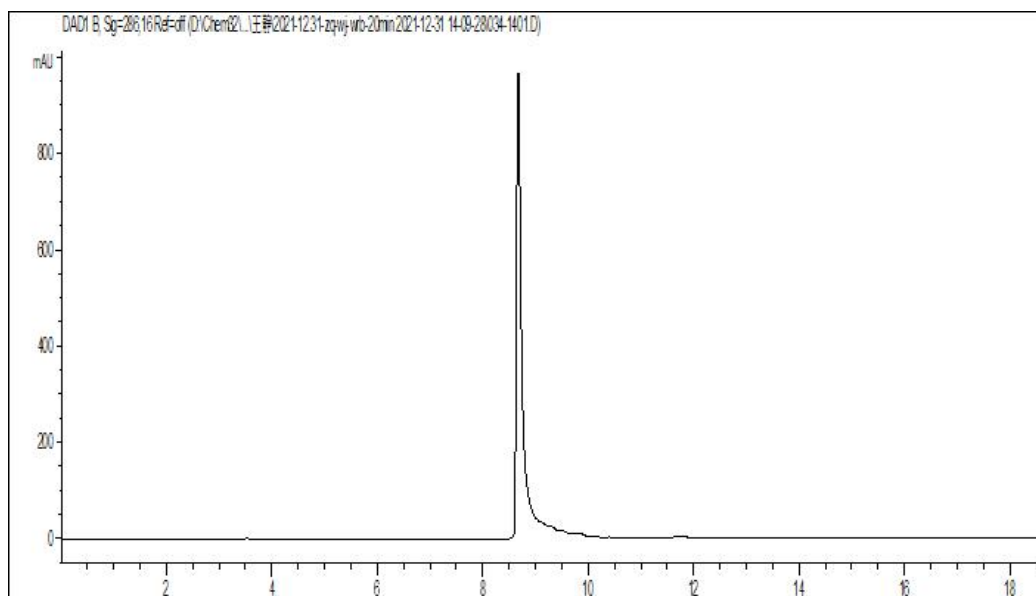


Figure S13. The HPLC of Ru(II)-2.

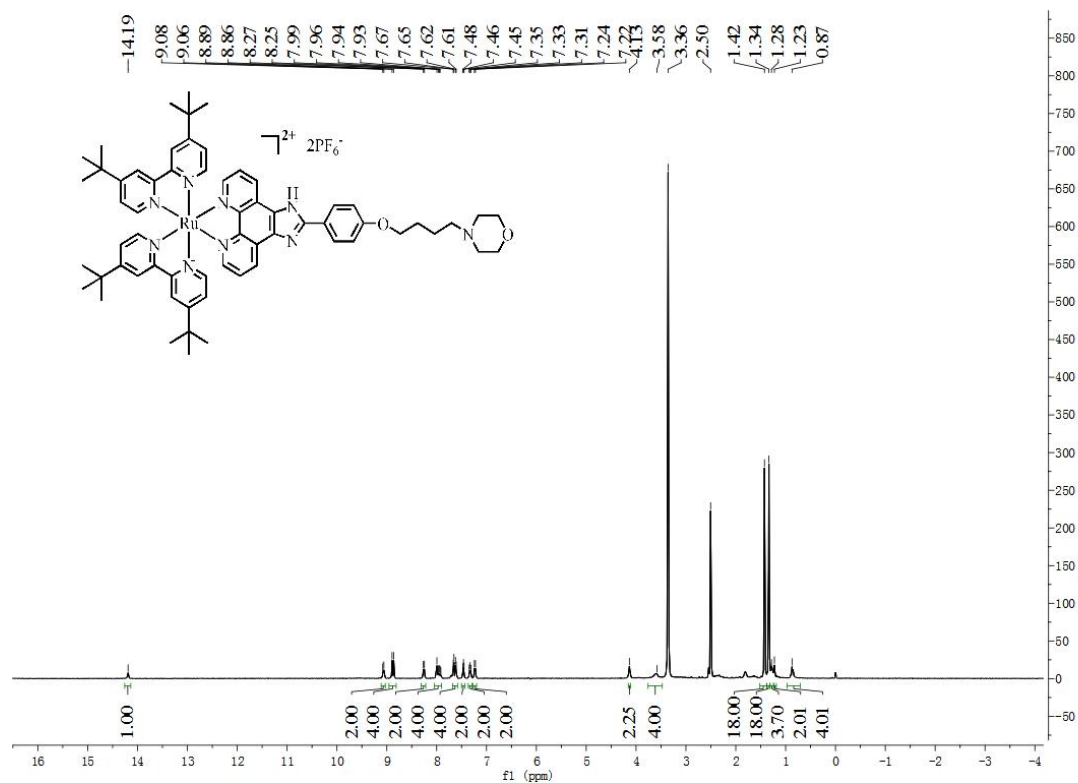


Figure S14. The ¹H NMR of Ru(II)-3.

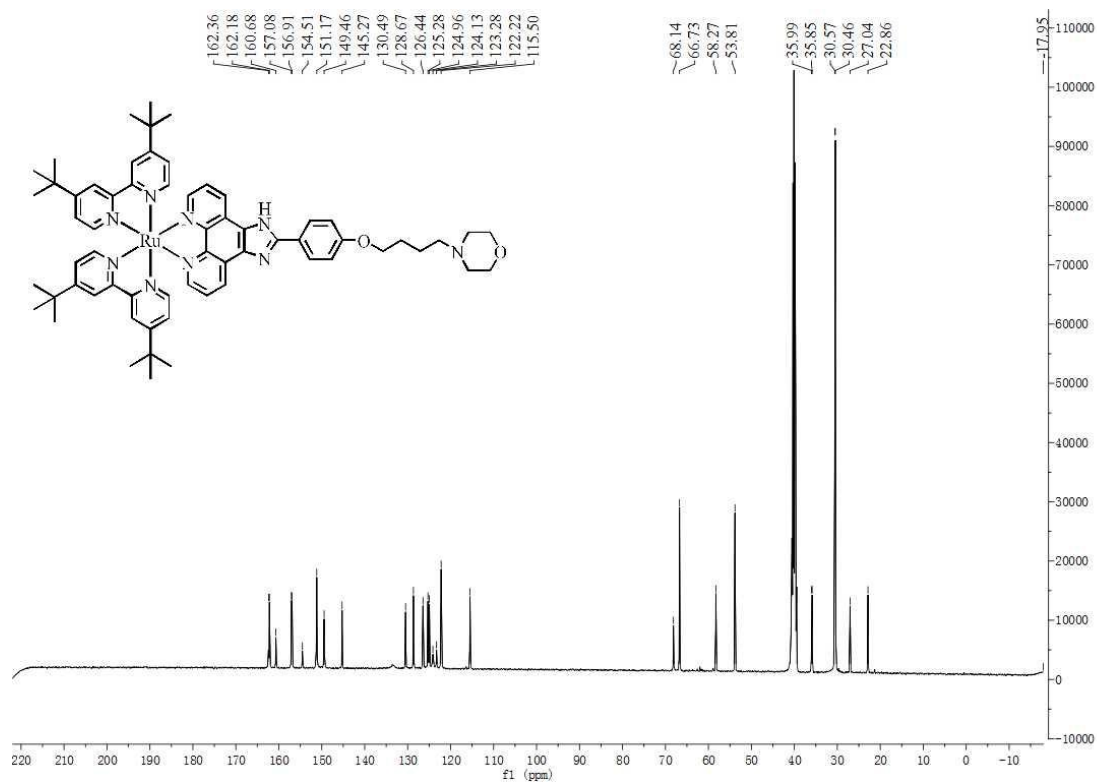


Figure S15. The ^{13}C NMR spectrum of the Ru(II)-3.

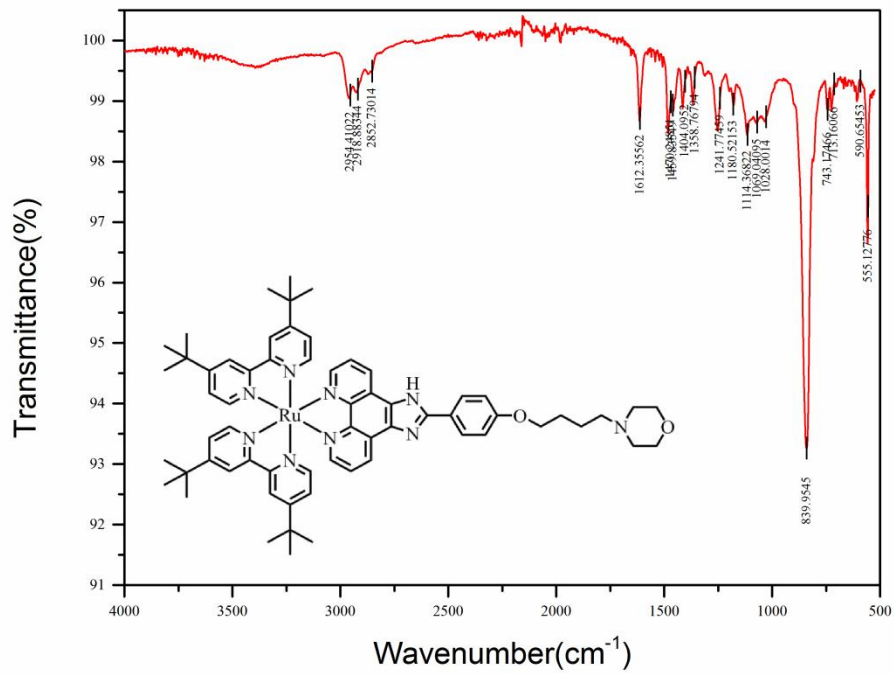


Figure S16. The IR spectrum of the Ru(II)-3

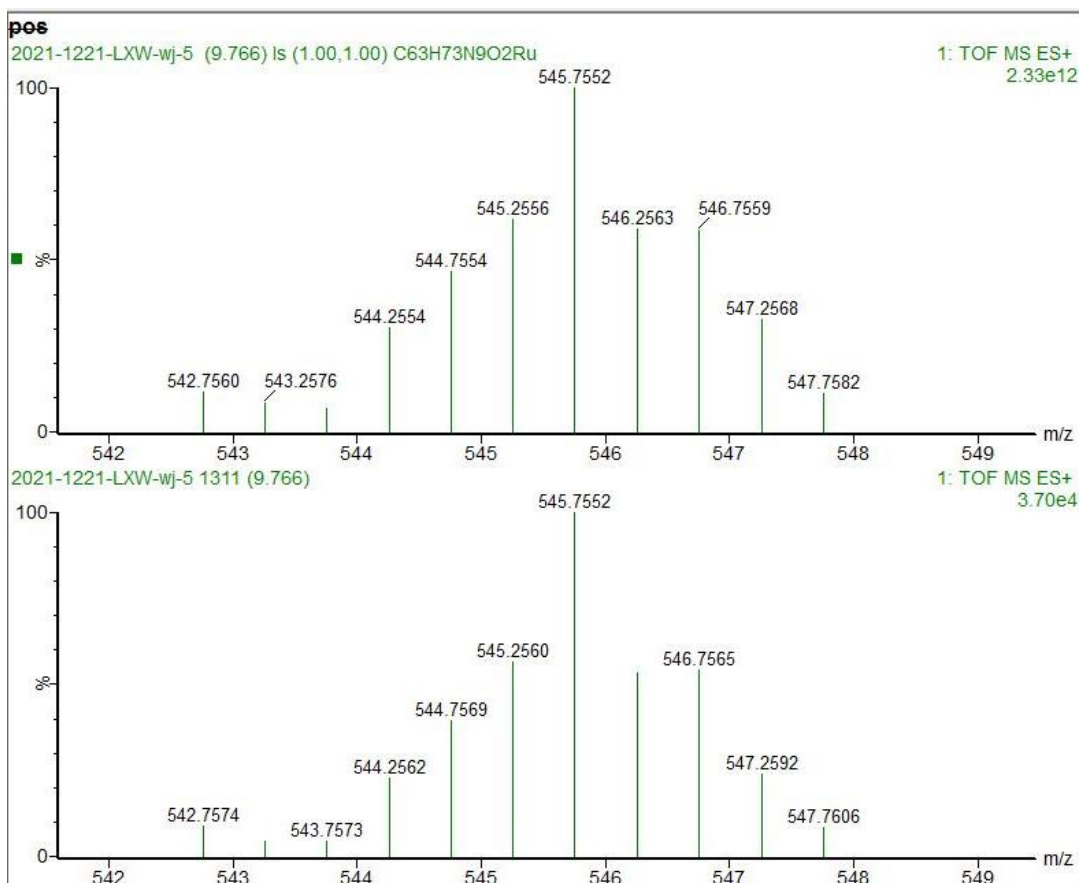


Figure S17. The HMRS of ligand **Ru(II)-3**.

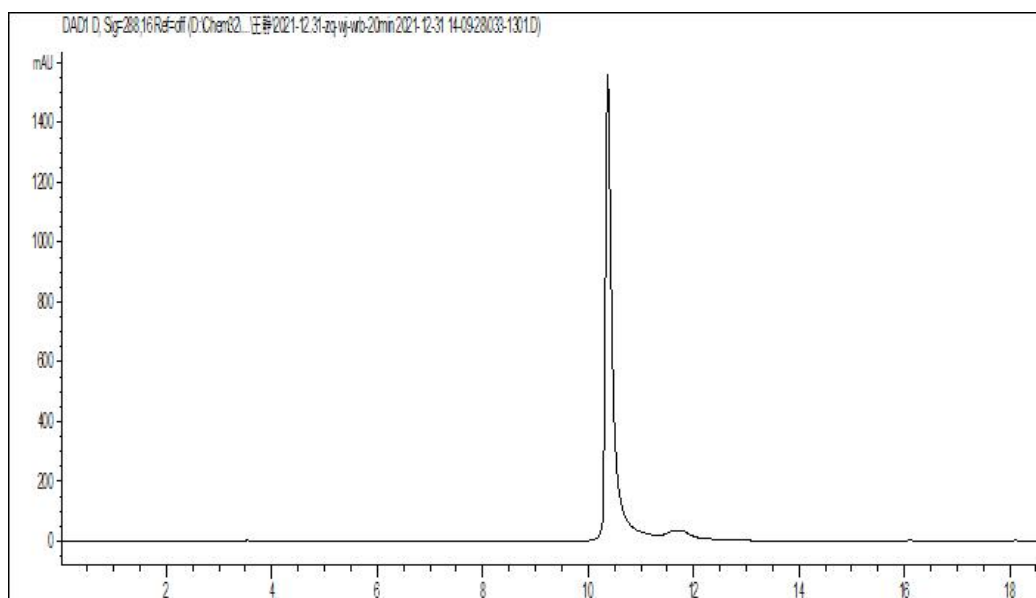


Figure S18. The HPLC of **Ru(II)-3**.

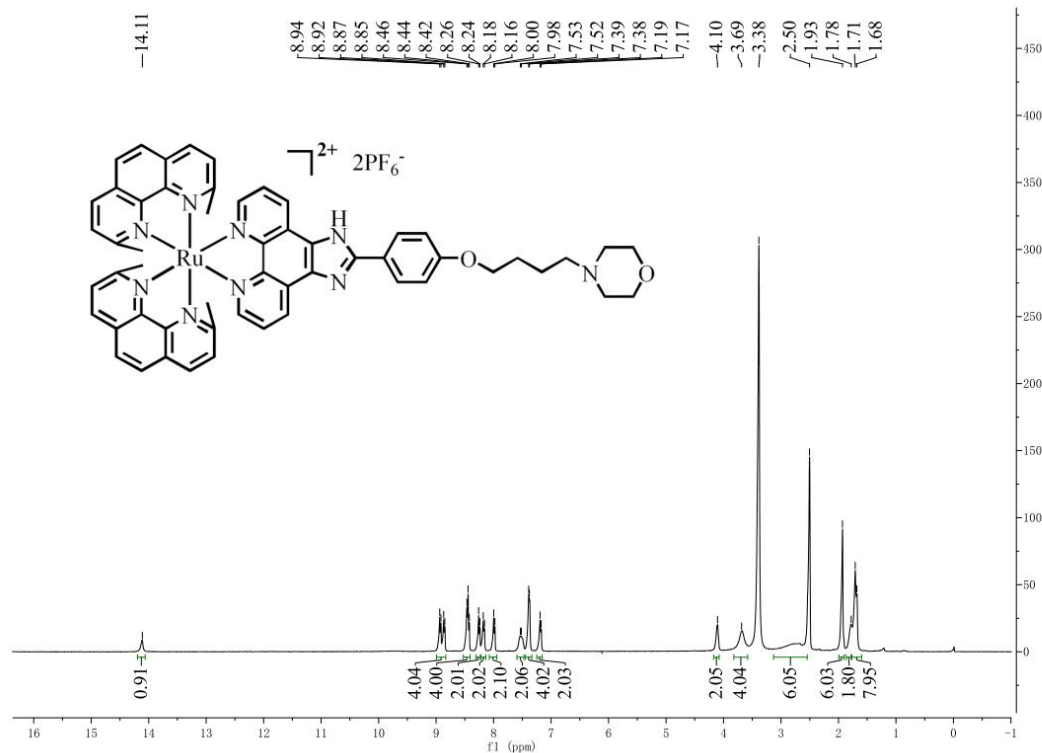


Figure S19. The 1H NMR of Ru(II)-4.

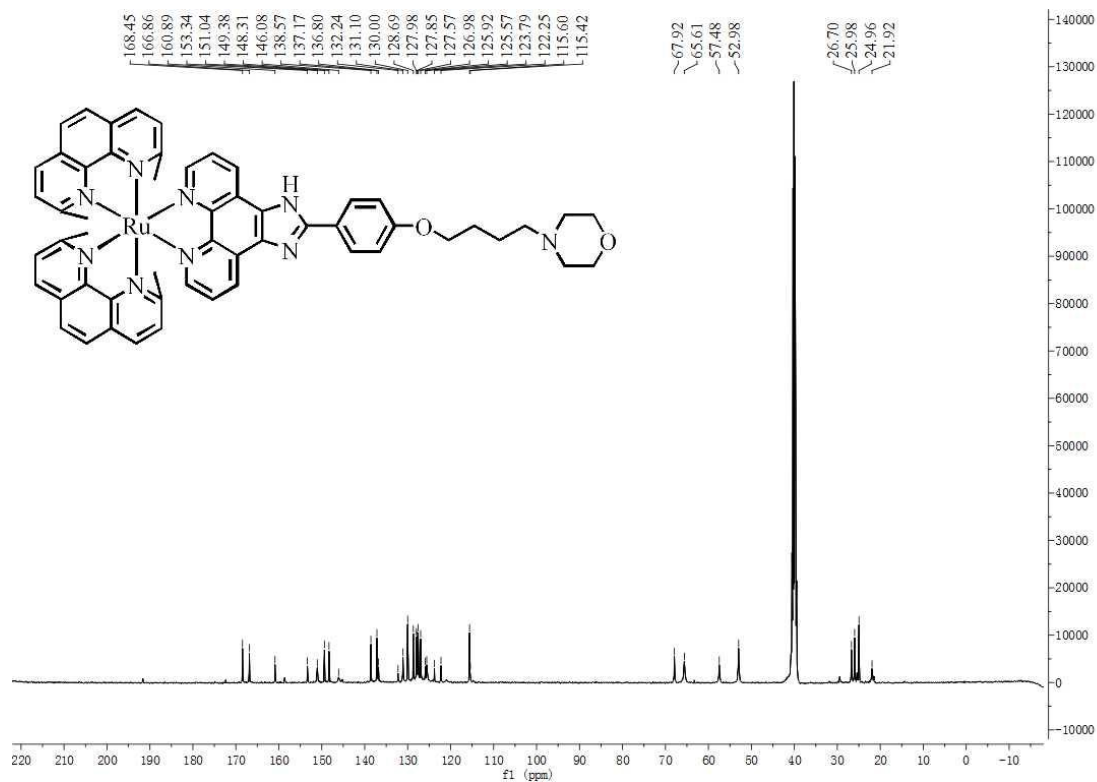


Figure S20. The ^{13}C NMR spectrum of the Ru(II)-4.

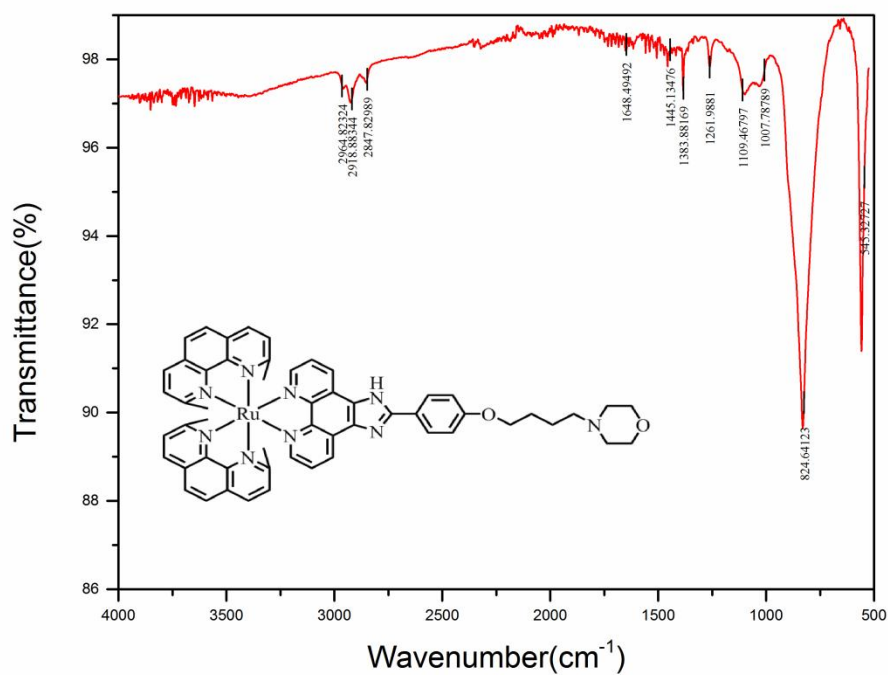


Figure S21. The IR spectrum of the Ru(II)-4

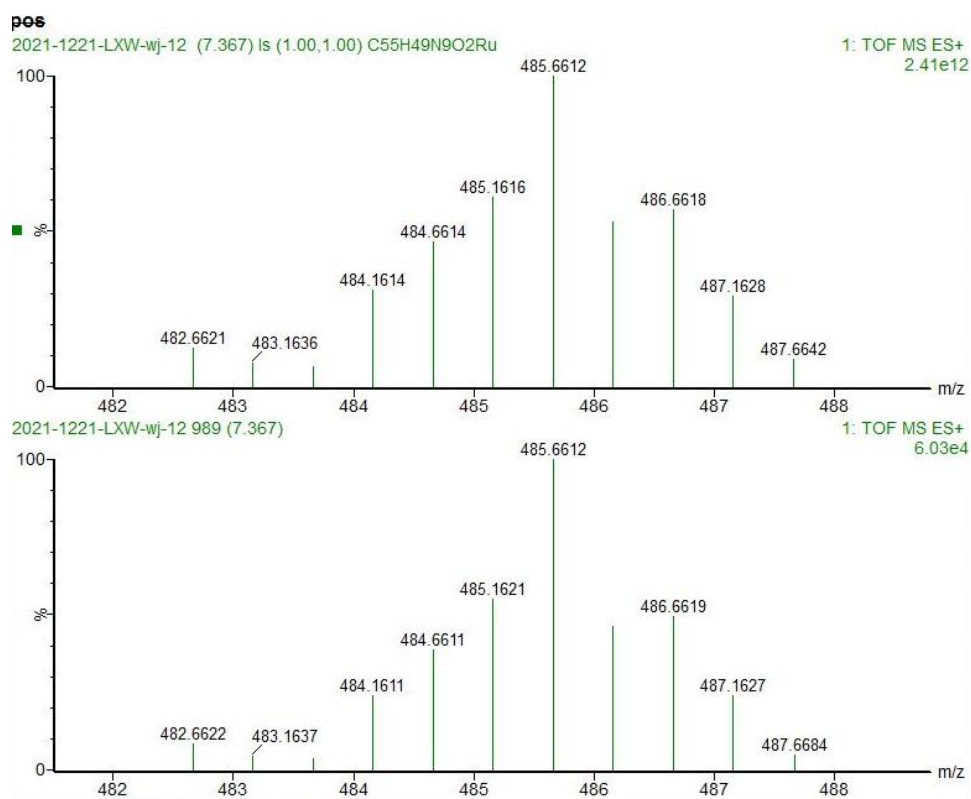


Figure S22. The HMRS of ligand Ru(II)-4.

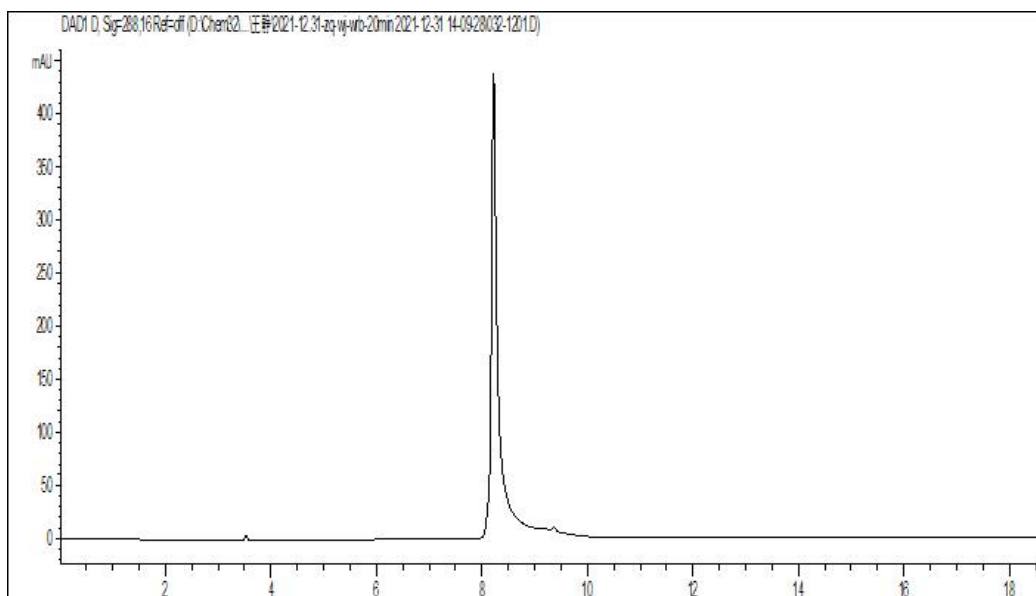


Figure S23. The HPLC of Ru(II)-4.

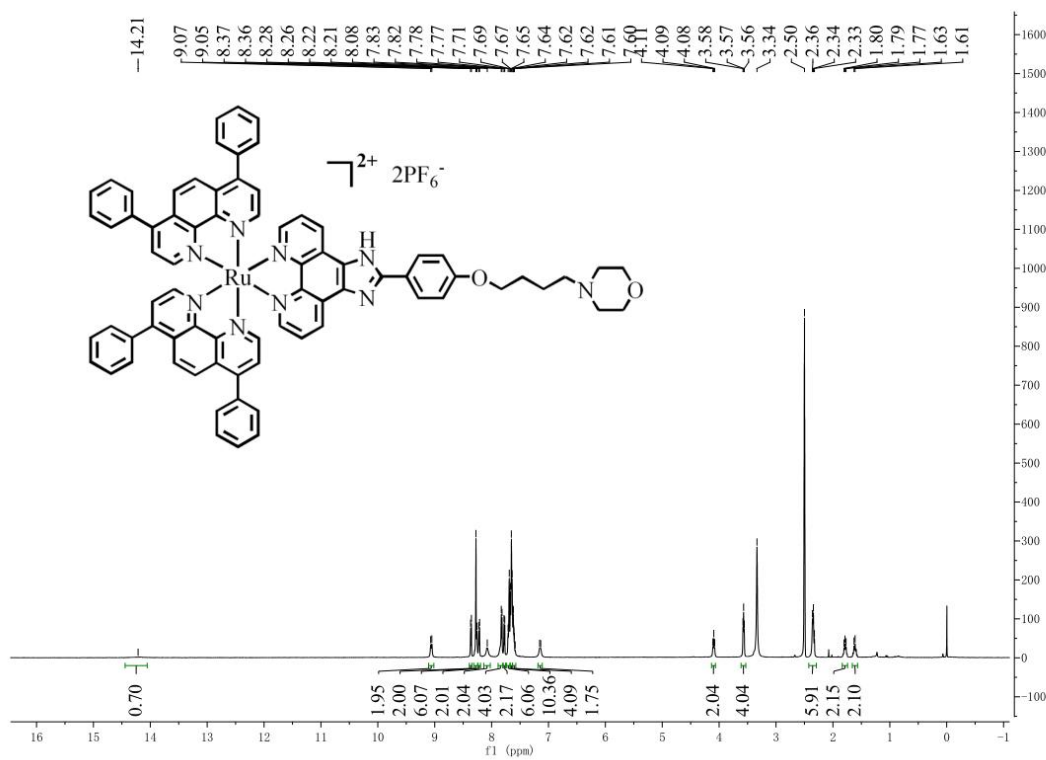


Figure S24. The ^1H NMR of Ru(II)-5.

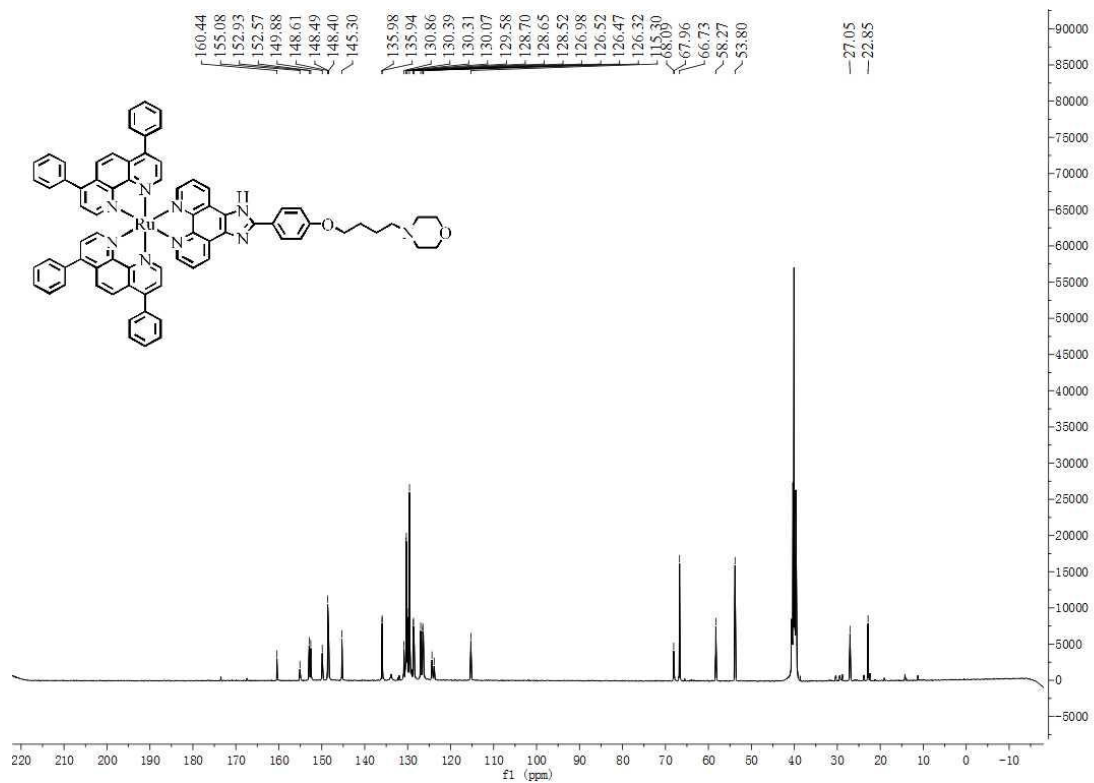


Figure S25. The ^{13}C NMR spectrum of the Ru(II)-5.

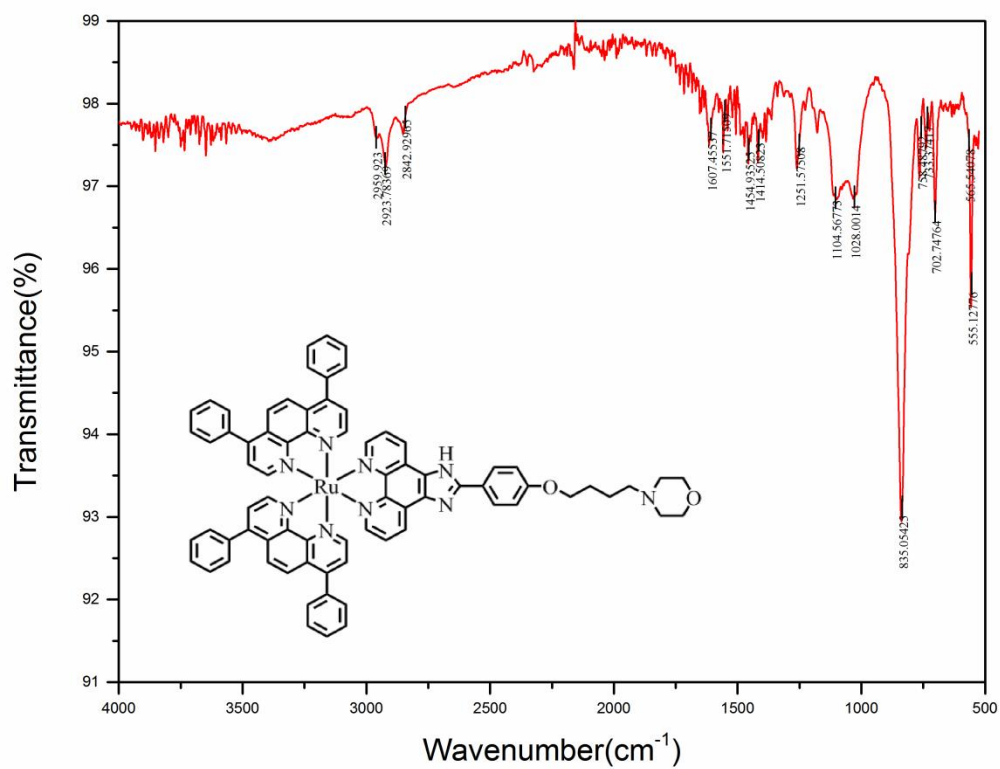


Figure S26. The IR spectrum of the Ru(II)-5

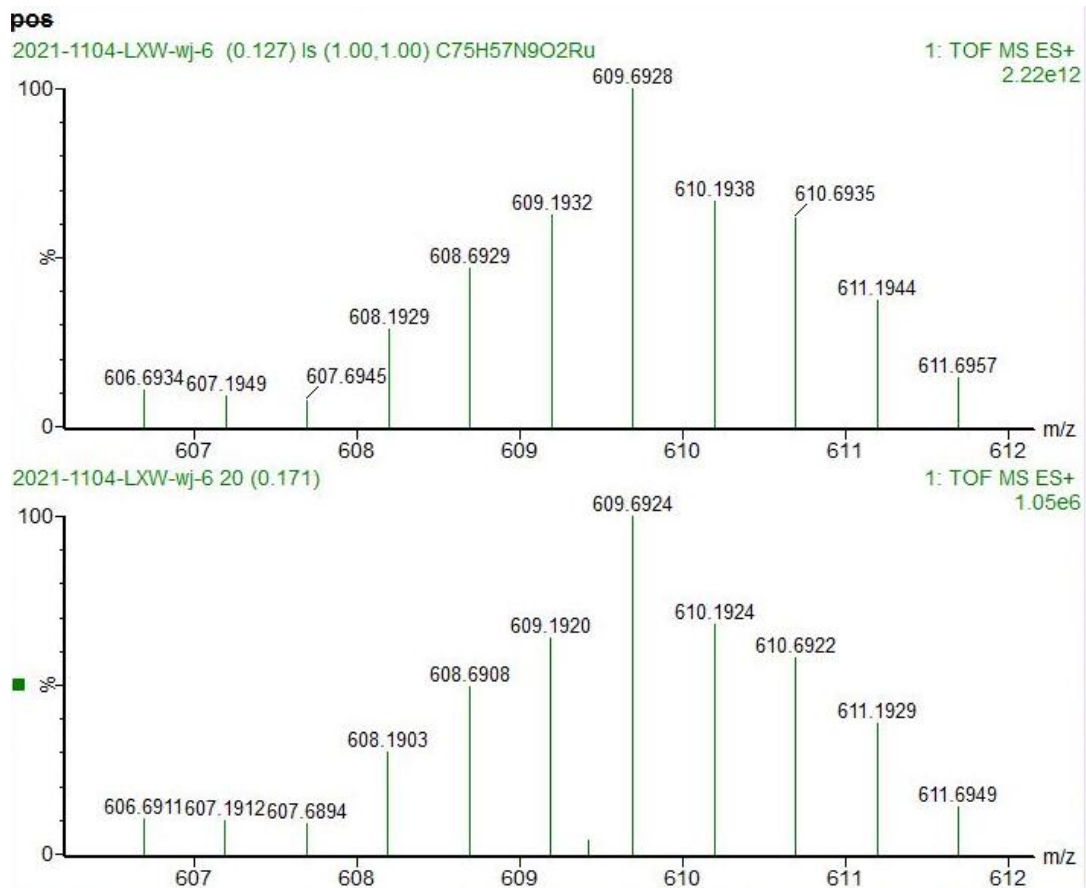


Figure S27. The HMRS of ligand Ru(II)-5.

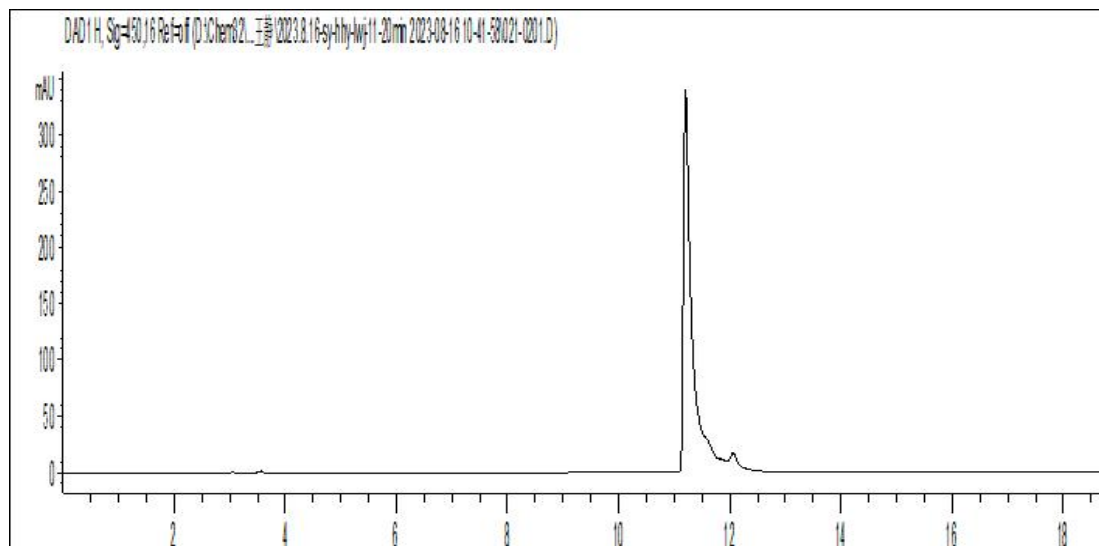


Figure S28. The HPLC of Ru(II)-5.

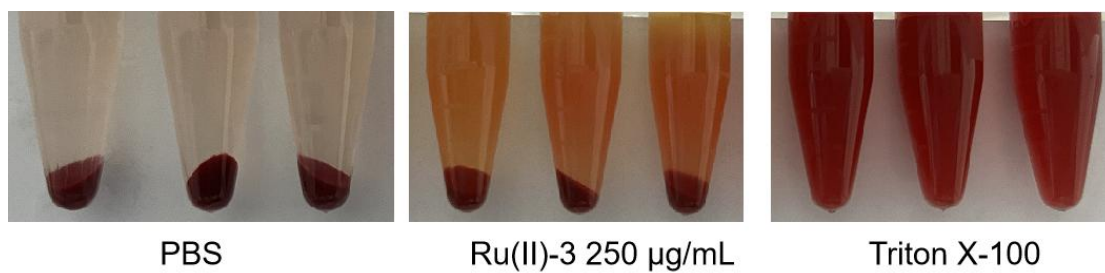


Figure S29. The images of the hemolytic effect of **Ru(II)-3** on rabbit blood cell.

Table S1. Minimum inhibitory concentration (MIC) values of **Ru(II)-3** against drug-resistant *S. aureus* (MRSA) isolated from the clinic.

Compound	MIC $\mu\text{g/mL}$
Ru(II)-3	0.2
Clindamycin	Resistance
Penicillin G	Resistance